A Bayesian Optimization Approach to Estimating Expected Match Time and Organ Quality in Kidney Exchange

Naveen Durvasula[†] and **Aravind Srinivasan**[‡] and **John P. Dickerson**[‡]
[†]Montgomery Blair High School [‡]University of Maryland
140.naveen.d@gmail.com, {srin,john}@cs.umd.edu

Abstract

Kidney exchanges allow patients with end-stage renal disease to find a lifesaving living donor by way of an organized market. However, not all patients are equally easy to match, nor are all donor organs of equal quality—some patients are matched within weeks, while others may wait for years with no match offers at all. Knowledge of expected waiting time and organ quality affects medical and insurance decisions. This work presents a principled method to estimate the expected quality of the kidney that a specific patient who enters an exchange will receive, as well as how long it will take to find that match. Estimation is performed via a novel Bayesian-optimization-based approach that learns a model of a computationally complex underlying Monte Carlo simulator. With a limited number of expensive simulation trajectories, the model produces results that are acceptable in practice. With access to fast and accurate sampling, medical professionals could have near-instantaneous access to valuable insight regarding a patient's expected outcome in a kidney exchange system.

1 Introduction

Renal disease affects millions of people worldwide, with a societal burden comparable to that of diabetes (Neuen et al. 2013). A patient with end-stage renal failure requires one of two treatments to stay alive: either frequent and costly filtration and replacement of their blood, known as dialysis, or the reception of a new organ via transplantation from a donor with one or more healthy kidneys. The latter option is often preferable due to increased quality of life and other health outcomes (Santos et al. 2015).

Donor kidneys are obtained from one of three sources: the deceased donor waiting list, where cadaveric kidneys are harvested from deceased donors with still-healthy kidneys; ad-hoc arrangement between a compatible living donor and a patient; and, recently, *kidney exchanges*, a type of organized market where patients swap willing donors with other needy patients (Roth, Sönmez, and Ünver 2004; 2005a; 2005b). Kidney exchanges, while still quite new, result in increased numbers and quality of transplants (Sönmez, Unver, and Yenmez 2017); furthermore, their design is a success story for fielded AI research (Abraham, Blum, and Sandholm 2007; Ashlagi and Roth 2014; Anderson et al. 2015; Dickerson and Sandholm 2015; Hajaj et al. 2015; Toulis and Parkes 2015; Manlove and O'Malley 2015).

The act of getting a kidney transplant is time sensitive, and affects healthcare and lifestyle decisions; furthermore, the expected quality of the kidney—if any—received by a patient affects the decision to accept or reject a particular match offer, and may be used to (de)prioritize patients in a matching mechanism (Bertsimas, Farias, and Trichakis 2013). Thus, decision support systems that incorporate donor and patient features and quantify or predict the value of a current or future offered kidney are valuable to practitioners. The Kidney Donor Profile Index (KDPI) (Rao et al. 2009) and the Living Kidney Donor Profile Index (LKDPI) (Massie et al. 2016) are well known and used to assess deceased- and living-donor kidneys, respectively. However, no method (nor system) currently exists to find the expected quality of a donated kidney in a kidney exchange.

This paper presents a Bayesian-optimization-based system that takes as input features of a patient and his or her paired donor and returns an estimate of (i) the expected quality of and (ii) expected waiting time for a matched kidney offer. The use of modern tools from machine learning and combinatorial optimization is required due to the NP-hard and APX-hard nature of even the most basic problems in kidney exchange (Abraham, Blum, and Sandholm 2007; Biró and Cechlárová 2007; Biró, Manlove, and Rizzi 2009; Luo et al. 2016; Jia et al. 2017). Our method uses a realistic but expensive black box Monte Carlo simulator to produce estimates of match quality and time to match for a specific patient and donor; it samples new points in the space intelligently, balancing overall computational time with the accuracy of prediction for a new patient and donor. That prediction can be done in real or near-real time, a requirement for such a decision support system. We give a proof of concept implementation on a reduced but realistic set of features in the kidney exchange setting, and show that the method learns the necessary functions well.

2 Preliminaries

In this section, we briefly overview terminology used in the allocation of kidneys to patients (§2.1), as well as the standard model of kidney exchange (§2.2).

2.1 Deceased- and Living-Donor Kidney Allocation

Our motivation in this paper is, in part, due to the widespread usage of the Kidney Donor Profile Index (KDPI) to quantify the value of deceased-donor kidneys, and the increasing use of the new Living Kidney Donor Profile Index (LKDPI) to quantify the value of living-donor kidneys (Rao et al. 2009; Massie et al. 2016). Roughly speaking, both the KDPI and the LKDPI are metrics used to compute the expected lifetime (quality) of a kidney that is donated from a donor D to a patient P. The LKDPI metric was constructed such that LKDPI scores can be directly compared with KDPI scores, thus allowing direct comparison between living donor and deceased donor options. We expand this metric of quality to fielded kidney exchange. Unlike a standard ad-hoc living-donor donation, in a donation through a kidney exchange, the features of the end donor are unknown, and are generated through a stochastic matching process. We aim to compute the expected LKDPI of the kidney received through kidney paired donation and the expected matching time that it would take to receive this kidney in order to allow for comparison between living donor, deceased donor, and kidney paired donation options.

Because we build on the LKDPI metric in this paper, we formally restate its calculation below.

$$\begin{aligned}\text{LKDPI}(D,P) = &-11.30\\ &+1.85 * [(D_{\textbf{age}} - 50) \textit{ if } D_{\textbf{age}} > 50]\\ &-0.381 * D_{\textbf{eGFR}}\\ &+1.17 * D_{\textbf{BMI}}\\ &\quad (+22.34 \textit{ if } D_{\textbf{is African-American}})\\ &\quad (+14.33 \textit{ if } D_{\textbf{has history of cigarette use}})\\ &+0.44 * D_{\textbf{systolic blood pressure}}\\ &\quad (-21.68 \textit{ if } D \textbf{ and } P \textbf{ are both male})\\ &\quad (+27.30 \textit{ if } D \textbf{ and } P \textbf{ are ABO incompatible})\\ &\quad (-10.61 \textit{ if } D \textbf{ and } P \textbf{ are unrelated})\\ &+8.57 * (\#\textbf{HLA-B mismatches})\\ &+8.26 * (\#\textbf{HLA-DR mismatches})\\ &-50.87 * \left[\min\left(\frac{D_{\textbf{weight}}}{P_{\textbf{weight}}}, 0.9\right)\right]\end{aligned}$$

Here, the estimated glomerular filtration rate (eGFR), body mass index (BMI), blood type (ABO) compatibility, and human leukocyte antigen (HLA) are all integral or real values determined by physical medical testing.[1]

2.2 The Formal Kidney Exchange Model

The most-used model represents a kidney exchange as a directed graph $G = (V, E)$, called a *compatiblity graph*. Here, each patient and paired donor who enter the pool are represented as a single vertex. Then, a directed edge is drawn from vertex v_i to vertex v_j if the patient at vertex v_j wants the donor kidney of vertex v_i. Weights $w_e \in \mathbb{R}$ represent the utility of an individual kidney transplant represented by an edge e, and are also used to (de)prioritize specific classes of patient (Dickerson, Procaccia, and Sandholm 2014; UNOS 2015).

Kidney exchanges rely on one of two types of structures to match patients: cycles and chains. First, a *k-cycle* c consists of exactly k patient-donor pairs (vertices), each connected by an edge in a cycle; here, each pair in c receives the kidney from the previous pair. Second, a *k-chain* begins with a non-directed donor, who enters the pool without a patient and gives her kidney to a patient with a paired donor, who gives to another patient with a paired donor, and so on k times.[2] Modern exchanges derive the majority of their utility from chains (Montgomery et al. 2006; Rees et al. 2009; Anderson et al. 2015; Ashlagi et al. 2017).

A *matching* M is a set of disjoint cycles and chains in a compatibility graph G; $M \in \mathcal{M}$, the set of all legal matchings. No donor can give more than one of her kidneys, necessitating the disjointness of cycles and chains—although recent work explores multi-donor donation (Ergin, Sönmez, and Ünver 2017; Farina, Dickerson, and Sandholm 2017). Given the set of all legal matchings $\mathcal{M}$, the *clearing problem* finds the matching M^* that maximizes utility function $u : \mathcal{M} \to \mathbb{R}$ (e.g., for maximum weighted matching, $u(M) = \sum_{c \in M} \sum_{e \in c} w_e$). Formally: $M^* \in \arg\max_{M \in \mathcal{M}} u(M)$. Ongoing research in the AI/Economics literature uses utility functions to enforce incentive properties via mechanism design (Ashlagi and Roth 2014; Li et al. 2014; Hajaj et al. 2015; Blum et al. 2017; Mattei, Saffidine, and Walsh 2017).

Finding a maximum weight (capped-length) cycle and chain packing is NP-hard (Abraham, Blum, and Sandholm 2007; Biró, Manlove, and Rizzi 2009), and is also hard to approximate (Biró and Cechlárová 2007; Luo et al. 2016; Jia et al. 2017). In practice, integer program (IP) formulations are used to clear large exchanges (Abraham, Blum, and Sandholm 2007; Dickerson, Procaccia, and Sandholm 2013; Glorie, van de Klundert, and Wagelmans 2014; Anderson et al. 2015; Dickerson et al. 2016). Formally, denote the set of all legal chains of length no greater than K and cycles of length no greater than L by $\mathcal{C}(L, K)$. Then, solve the following integer program:

$$\max \sum_{c \in \mathcal{C}(L,K)} w_c \, x_c \qquad s.t. \qquad \sum_{c : v \in c} x_c \leq 1 \quad \forall v \in V,$$

where $x_c \in \{0, 1\}$ is a binary variable for every $c \in \mathcal{C}(L, K)$, and $w_c = \sum_{e \in c} w_e$. The final matching is the set of chains and cycles c such that $x_c = 1$. We use this integer program as a subsolver in this work.

The kidney exchange system is dynamic. In each time iteration, new patients enter the pool, current patients may

[1] While we direct the reader to the medical literature for a full explanation of all variables in this equation (Massie et al. 2016), we overview ABO compatibility here. At a high level, blood is partitioned into four types: O, A, B, and AB. Blood type O, known as the "universal donor" type, can be donated to patients of any other blood type. Blood types A and B can be donated to types A and B, respectively, along with type AB; blood type AB can be donated only to those of type AB blood. A donor whose blood type can be donated to a patient is said to be an *ABO compatible* donor.

[2] In fielded kidney exchanges, cycles are limited in size to, typically, 3; all surgeries in a cycle must be executed simultaneously, so longer cycles are nearly impossible to plan. Chains, however, can be much longer (or effectively endless) in practice.

leave the pool due to competition with other methods for receiving a kidney or death.

The matching process itself is highly stochastic. In fielded kidney exchanges, matches are made without detailed knowledge of the pairwise compatibility between a donor and patient. More thorough *cross-match tests* are done post-match to ensure that a matched donor can donate to a paired patient. Just one failure can invalidate a cycle or stop a chain from continuing. The process of patients entering and leaving as described above adds introduces further noise to the system.

3 Estimating additive functions of expensive stochastic processes

In this section, we formally specify our model for quantifying the quality of an organ, as well as our method for predicting the expected quality of that organ given a black box exchange simulator. As defined, the model and method are applicable to any additive function of a stochastic simulatable process; however, given our application, we motivate the model in the context of kidney exchange.

Consider a *stochastic process* $\mathbb{S}(\mathbf{I}) \rightarrow \mathbf{M}$ which produces output samples $\mathbf{M}$ given some input features $\mathbf{I}$. Let $\mathbf{I} \in \mathcal{I}, \mathbf{M} \in \mathcal{M}$, where $\mathcal{I}$ denotes the *input space* and $\mathcal{M}$ denotes the *output space*.

Example 1 *In this application, let $\mathbb{S}$ denote the kidney exchange process as described in Section 2. We compute samples from $\mathbb{S}$ by constructing a realistic simulator. Let $\mathbf{I}$ denote the feature set of a patient-donor pair that enters the system. Let $\mathbf{M}$ be a set containing the feature set of the donor that gets matched to the patient of $\mathbf{I}$ and the total time taken for $\mathbf{I}$ to be matched. The simulator will be discussed in more detail in section 4.*

Let a function $f(\mathbf{x})$ have additive structure if and only if

$$f(\mathbf{x}) = \sum_k f_k(\mathbf{x}) \tag{1}$$

Consider some stochastic additive function $f(\mathbf{I}, \mathbf{M}|\mathbf{I})$, with $\mathbf{M}$ and $\mathbf{I}$ as defined above. The notation $\mathbf{M}|\mathbf{I}$ is used to show that $\mathbf{M}$ is not a real input to the function - the function depends only on $\mathbf{I}$ as $\mathbf{M} = \mathbb{S}(\mathbf{I})$. However, to compute f, we require samples of $\mathbf{M}$. Let $F(\mathbf{I}) = \mathrm{E}[f(\mathbf{I}, \mathbf{M}|\mathbf{I})]$.

Example 2 *In our running example, let*

$$f(\mathbf{I}, \mathbf{M}|\mathbf{I}) = \mathrm{LKDPI}(\mathbf{M}|\mathbf{I}, \mathbf{I})$$

return the LKDPI *of the kidney that the patient of the patient-donor pair $\mathbf{I}$ receives through matching. Note that by the* LKDPI *formula, f is an additive function. Let $F(\mathbf{I})$ return $\mathrm{E}[\mathrm{LKDPI}(\mathbf{M}|\mathbf{I}, \mathbf{I})]$ respectively. Let $t(\mathbf{I})$ be a stochastic function that returns the matching time for patient-donor pair $\mathbf{I}$. Let $T(\mathbf{I}) = \mathrm{E}[t(\mathbf{I})]$. While the t function does not decompose into some additive components, we treat it as a degenerate additive function with only one component. We aim to approximate and provide patients with reasonable estimates for $F(\mathbf{I})$ and the expected matching time $T(\mathbf{I})$ for patient-donor pair $\mathbf{I}$. We could always sample from $\mathbb{S}(\mathbf{I})$ for a sufficient number of trajectories, and use this to estimate $F(\mathbf{I})$ and $T(\mathbf{I})$. However, this becomes computationally intractable very quickly if $\mathbb{S}$ simulates a sufficiently noisy and/or time consuming process. In this application, output samples of $\mathbf{M}$ are very noisy, and even the basic matching policy described in Section 2 is computationally intractable if a sufficient number of samples are taken to accurately compute $F(\mathbf{I})$ and $T(\mathbf{I})$. This estimation strategy becomes even less feasible if more advanced matching policies that use reinforcement learning methods (Dickerson and Sandholm 2015) are used.*

Note that in the above formulation, we place no constraints on the behavior of f_k. Thus, trying to learn F directly is also difficult due to the fact that it may not be continuous. We note that F also has an additive structure. We exploit this additive structure in order to effectively learn F.

$$\begin{aligned} F(\mathbf{I}) &= \mathrm{E}[f(\mathbf{I}, \mathbf{M}|\mathbf{I})] \\ &= \mathrm{E}\left[\sum_k f_k(\mathbf{I}_k, \mathbf{M}_k|\mathbf{I}_k)\right] \\ &= \sum_k \mathrm{E}[f_k(\mathbf{I}_k, \mathbf{M}_k|\mathbf{I}_k)] \\ &= \sum_k F_k(\mathbf{I}_k) \end{aligned} \tag{2}$$

Where $\mathbf{M}_k \subseteq \mathbf{M}, \mathbf{I}_k \subseteq \mathbf{I}$, and both $\mathbf{I}_k$ and $\mathbf{M}_k$ are of the smallest size possible. Note that while elements of $\mathbf{M}_k$ can be reduced to only those that are required for computing f_k, the elements of $\mathbf{I}_k$ must be sufficient to compute $\mathbf{M}_k$ and f_k. In other words, if $\mathbf{I}_k \neq \mathbf{I}$, it must be a property of $\mathbb{S}$ that the elements of $\mathbf{I} \setminus \mathbf{I}_k$ do not alter the joint probability distribution $p(\mathbf{M}_k)$ over the elements of $\mathbf{M}_k$.

Not all F_k are equally difficult to estimate. Consider the case where no elements of $\mathbf{I}$ change $p(\mathbf{M}_k)$. If this occurs, we can estimate F_k by first estimating $p(\mathbf{M}_k)$ by sampling from $\mathbb{S}(*)$ and integrating

$$F_k(\mathbf{I}_k) = \int_{\mathbf{M}_k} \cdots \int f_k\left(\mathbf{I}_k, \bigcup_i \mathbf{M}_k^i\right) p\left(\bigcup_i \mathbf{M}_k^i\right) \prod_{i=1}^{l} d\mathbf{M}_k^i \tag{3}$$

where $\mathbf{M}_k = \bigcup_i \mathbf{M}_k^i$.

However, if F_k does not fall in this case, we present a Bayesian optimization based technique to learn F_k which requires the use of $\mathbb{S}$ to generate samples.

3.1 Bayesian optimization as an active learning method

Bayesian optimization (BO) utilizes Gaussian Processes (GP) to maximize an unknown function, in this case, the expected output of a realistic simulator. The acquisition function is used to select the best point on the function to sample that would lead us to the absolute maximum. Examples include Expected Improvement (EI), Lower Confidence Bound (LCB), and Maximum Probability of Improvement (MPI); Brochu, Cora, and De Freitas (2010) give an in-depth overview of techniques. A kernel (covariance) function is used to interpolate between known values of the function,

and determine the confidence at each point. While BO offers a method to maximize a function where getting output is time consuming, we learn F_k using this method by taking as output the GP of the BO. We use the Bayesian optimization framework to choose informative values of $\mathbf{I}_k$ which will increase our understanding of F_k.

More formally, we let

$$f_k \sim \mathcal{GP}(\mu(\mathbf{I}_k), \mathrm{k}(\mathbf{I}_k, \mathbf{I}'_k)) \tag{4}$$

where $\mathrm{k}(\mathbf{I}_k, \mathbf{I}'_k)$ is a kernel (covariance) function. To learn a function using BO, we let the acquisition function $A(\mathbf{I}_k)$ return the variance at the point. By equation (4), we have

$$p(f_k(\mathbf{I}_k)) = \mathcal{N}(\mu_{\mathbf{I}_k}, \sigma^2_{\mathbf{I}_k}) \tag{5}$$

We let

$$A(\mathbf{I}_k) = \sigma^2_{\mathbf{I}_k} \tag{6}$$

We optimize A using the limited-memory BFGS optimization algorithm (Andrew and Gao 2007). It follows that

$$F_k(\mathbf{I}_k) = \mu_{\mathbf{I}_k} \tag{7}$$

Accounting for categorical variables $\mathbf{I}_k$ may contain some categorical variables (in our example we have blood type). Because of this, we cannot directly apply a GP over $\mathbf{I}_k$, as we cannot fit a kernel over these categorical variables. Instead, for each permutation of categorical variables, we perform this scheme over $\mathrm{C}(\mathbf{I}_k)$, the subset of $\mathbf{I}_k$ containing only non-categorical variables. We let $\mathrm{D}(\mathbf{I}_k)$ be the subset containing only the categorical variables. We can compute F_k as

$$F_k(\mathbf{I}_k) = \mu^{\mathrm{D}(\mathbf{I}_k)}_{\mathrm{C}(\mathbf{I}_k)} \tag{8}$$

Where the notation $\mu^{\mathrm{D}(\mathbf{I}_k)}_{\mathrm{C}(\mathbf{I}_k)}$ denotes the mean at the point $\mathrm{C}(\mathbf{I}_k)$ on the GP conditioned on the categorical variables being set to $\mathrm{D}(\mathbf{I}_k)$.

Piecewise functions A special class of functions f_k for which a GP is not well suited to model are piecewise functions. Let f_k be a piecewise function with c cases.

$$f_k(\mathbf{I}_k, \mathbf{M}_k|\mathbf{I}_k) = \begin{cases} f^1_k(\mathbf{I}_k, \mathbf{M}_k|\mathbf{I}_k), & \textit{if } C^1_k(\mathbf{I}_k, \mathbf{M}_k|\mathbf{I}_k) \\ f^2_k(\mathbf{I}_k, \mathbf{M}_k|\mathbf{I}_k), & \textit{if } C^2_k(\mathbf{I}_k, \mathbf{M}_k|\mathbf{I}_k) \\ \vdots & \vdots \\ f^c_k(\mathbf{I}_k, \mathbf{M}_k|\mathbf{I}_k), & \textit{otherwise} \end{cases}$$

where each function $C^i_k(\mathbf{I}_k, \mathbf{M}_k|\mathbf{I}_k)$ is a mutually exclusive boolean valued function. We use the above scheme to learn each of the $F^i_k(\mathbf{I}_k) = \mathrm{E}[f^i_k(I_k, M_k)]$ as well as $\Pr[C^i_k(\mathbf{I}_k, \mathbf{M}_k|\mathbf{I}_k)]$ for $1 \leq i \leq c$.

We compute F_k as

$$F_k(\mathbf{I}_k) = \sum_{i=1}^{c} \Pr[C^i_k(\mathbf{I}_k, \mathbf{M}_k|\mathbf{I}_k)] F^i_k(\mathbf{I}_k) \tag{9}$$

by linearity of expectations.

Example 3 *The* LKDPI *function has several constituent terms that are defined by a piecewise function. One example is the term containing donor's BMI. Let the condition **AA** denote that the donor is African-American. Let the condition **HCU** denote that the donor has a history of cigarette use. We can write this term as*

$$f_3(\mathbf{I}_3, \mathbf{M}_3) = \begin{cases} 1.17 * (D_{\textbf{\textit{BMI}}} + 36.67), & \textit{if } \textbf{\textit{AA}} \wedge \textbf{\textit{HCU}} \\ 1.17 * (D_{\textbf{\textit{BMI}}} + 22.34), & \textit{if } \textbf{\textit{AA}} \\ 1.17 * (D_{\textbf{\textit{BMI}}} + 14.33), & \textit{if } \textbf{\textit{HCU}} \\ 1.17 * D_{\textbf{\textit{BMI}}}, & \textit{otherwise} \end{cases}$$

Defining the kernel For this application, we use the radial basis function (RBF) kernel for all GPs, given by

$$\mathrm{k}(\mathbf{I}_k, \mathbf{I}'_k) = \exp\left(-\frac{\|\mathbf{I}_k - \mathbf{I}'_k\|^2}{2\ell^2}\right) \tag{10}$$

The kernel is only accurate if the ℓ length-scale hyperparameter is properly tuned. We use Hamiltonian Monte Carlo (HMC) to approximate the probability distribution over ℓ given the data that we have seen so far.

HMC is a physics-inspired Markov Chain Monte Carlo (MCMC) technique. As the underlying distribution over ℓ is inaccessible, we construct a Markov chain which has an equilibrium distribution equal to the target distribution over ℓ. Sampling from this Markov chain allows us to efficiently explore the *typical set* of the underlying distribution. What makes HMC different from other MCMC methods such as the Metropolis-Hastings algorithm is its ability to smoothly explore the typical set without failing due to random walk behavior (Betancourt 2017). HMC accomplishes this by defining a vector field over the underlying distribution.

Just taking the gradient of the distribution gives a vector field that points towards the mode of the distribution. However, we want to make this vector field guide the Markov chain through the typical set. This is analogous to a physical system where we have a gravitational center, and we are trying to determine the *momentum* required to carry an object into orbit. We redefine our terminology in terms of the analogy. We let our *position* $\mathbf{q}$ be given by a coordinate of the density function. In our implementation of HMC, $\mathbf{q} = \ell$. The momentum parameter $\mathbf{p}$ is defined as an auxiliary parameter over our density function $p(\mathbf{q})$, and has the same dimension as $\mathbf{q}$. We call this augmented space over $\mathbf{q}$ and $\mathbf{p}$ the *phase space*.

We choose a conditional distribution $p(\mathbf{p} \mid \mathbf{q})$ because we can marginalize out the momentum, as

$$p(\mathbf{q}, \mathbf{p}) = p(\mathbf{p} \mid \mathbf{q}) p(\mathbf{q})$$

We can write this conditional distribution in terms of an invariant *Hamiltonian* function $H(\mathbf{q}, \mathbf{p})$ as

$$p(\mathbf{q}, \mathbf{p}) = e^{-H(\mathbf{q}, \mathbf{p})} \tag{11}$$

We refer to the value of the Hamiltonian at a given point within the phase space as the *energy* at that point. From the above, we have

$$\begin{aligned} H(\mathbf{q}, \mathbf{p}) &= -\log(p(\mathbf{q}, \mathbf{p})) \\ &= -\log(p(\mathbf{p} \mid \mathbf{q})) - \log(p(\mathbf{q})) \\ &\equiv K(\mathbf{p}, \mathbf{q}) + V(\mathbf{q}) \end{aligned} \tag{12}$$

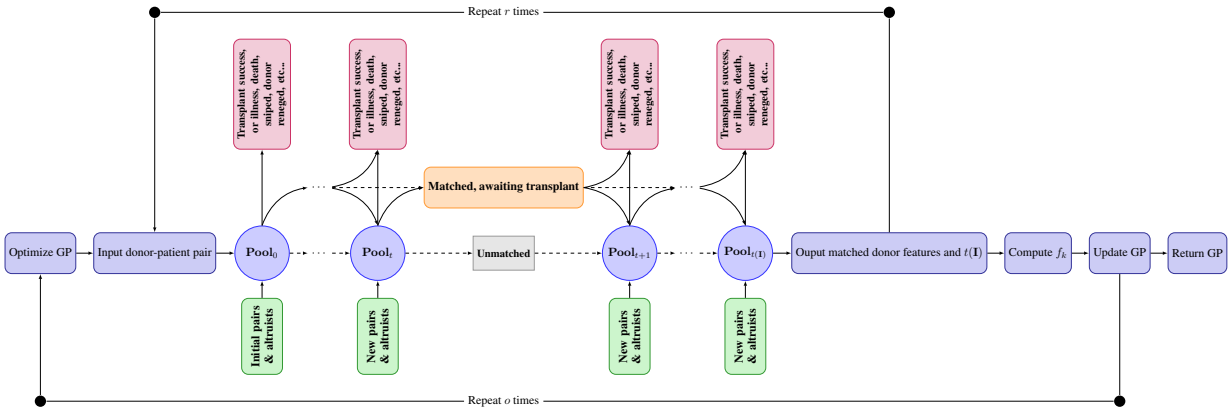

Figure 1: Estimating F_k or $T(\mathbf{I})$ using BO

We refer to K as the *kinetic energy*, and V as the *potential energy*. We can generate a vector field oriented with the typical set using *Hamilton's equations*, given by

$$\begin{aligned} \frac{d\mathbf{p}}{dt} &= \frac{\partial H}{\partial \mathbf{p}} = \frac{\partial K}{\partial \mathbf{p}} \\ \frac{d\mathbf{q}}{dt} &= -\frac{\partial H}{\partial \mathbf{q}} = \frac{\partial K}{\partial \mathbf{q}} - \frac{\partial V}{\partial \mathbf{q}} \end{aligned} \tag{13}$$

We let

$$p(\mathbf{p} \mid \mathbf{q}) = \mathcal{N}(\mathbf{p} \mid 0, M) \tag{14}$$

and thus define a *Euclidean-Gaussian* kinetic energy

$$K(\mathbf{p}, \mathbf{q}) = \frac{1}{2}\mathbf{p}^\intercal M^{-1}\mathbf{p} + \log|M| + \text{const.} \tag{15}$$

where M is defined by rotating a scaling a matrix of Euclidean inner products. We direct the reader to a more in depth explanation of Hamiltonian Monte Carlo (Betancourt (2017)) for more information.

We modify our acquisition function A to compute the expected value $\mathrm{E}[\sigma^2_{\mathbf{I}_k}]$ over the kernel's ℓ distribution.

$$A(\mathbf{I}_k) = \int_0^\infty (\sigma^2_{\mathbf{I}_k} | \ell) p(\ell) d\ell \tag{16}$$

4 Experimental Setup

We instantiate the model under a simplified kidney exchange process. The only factors that affect $p(\mathbf{M})$ under this matching policy are

- Patient Blood Type
- Paired Donor Blood Type
- Patient CPRA

Here, the Calculated Panel Reactive Antibodies (CPRA) is a score in $[0, 1]$ roughly representing the fraction of donors, drawn from a general population, that would *not* be a match for a particular patient (i.e., a CPRA score of 1 signals extreme difficulty in matching).

The consequence of using the simplified kidney exchange process is that the only one of these factors which appear in the LKDPI formula is patient blood type. Furthermore, it only appears in the form of a comparison between the matched donor's blood type and the patient's blood type. $\mathcal{C}(L, K)$ as mentioned in Section 2 only contains cycles and chains where the matched donor has the same blood type as the patient. Thus, all F_k can be computed by equation (3). We evaluate the BO approach by estimating the expected matching time $T(\mathbf{I})$. We let $\mathcal{I}$ be the space over the features listed above. To reduce noise on the output of $\mathbb{S}$, we compute r samples of $\mathbb{S}(\mathbf{I})$ each optimization iteration. We let matches take place on a weekly basis, and cap the total match time at 250 weeks. We perform o optimization iterations. Figure 1 describes the instantiation of the BO approach for LKDPI computation.

4.1 Bayesian Optimization for Match Time Computation

We use GPyOpt (2016), an open source Bayesian optimization platform for Python as the base for implementing the described method. We modified GPyOpt to change the acquisition to return the integrated expected variance at the point as described in section 3. Then, for all 16 blood type pair combinations for patient-donor pairs who enter the exchange, we performed Bayesian optimization over patient CPRA for $o = 50$ iterations. For each blood type pair combination, $T(\mathbf{I})$ is estimated based on $r = 48$ trajectories in a realistic simulator.

We now experimentally validate the proposed method using a realistic kidney exchange simulator and a reduced feature set, as a proof of concept. In practice, one would include 25-30 features before making a policy recommendation; however, as section 5 will show, even using a reduced feature set validates the method.

After constructing the Gaussian processes (GPs) through BO, we tested them by comparing the match time returned by the GP and the match time returned by the realistic simulator after s trajectories. To test the 16 generated GPs, the domain of CPRA $[0, 1]$ is partitioned uniformly into 4 zones $\{[0, .25), [.25, .5), [.5, .75), [.75, 1)\}$. In each zone, 5 random trials are done, with $s = 128$ trajectories each.

5 Experimental Results

We briefly overview our experimental results. Figure 2 shows the estimated expected mean residual of our estimated function when compared to our simulated test of the value of that function in weeks, calculated over all blood type combinations. First, the learned function fits the true (simulated) function quite well, for CPRA values far from 1. As the CPRA value approaches 1, the residuals increase; this is to be expected, because higher CPRA values result in more uncertainty in the ability to find any match at all. Indeed, a CPRA of 1 indicates zero probability of finding a match; in a case like this, waiting time becomes infinity, and the function to be estimated becomes ill-defined. To prevent the simulation from taking an indefinite amount of time, we cap the total match time at 250 weeks.

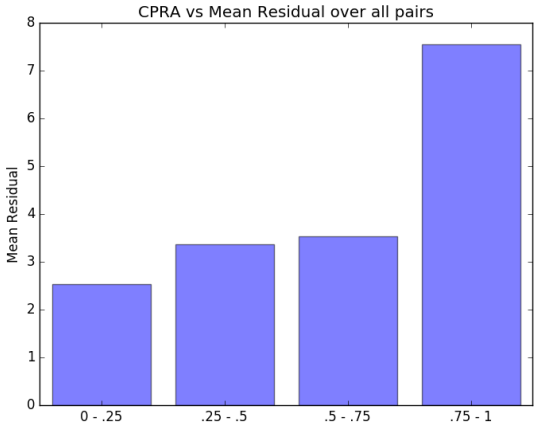

Figure 2: Mean residual in weeks over all blood type pairs

Figure 3 shows the distribution on the function mapping patient CPRA for the blood type combination O-AB in weeks, the acquisition function (in red) in arbitrary units, and the point at which the acquisition is optimized (the solid red line going down). We see that uncertainty is quite low, even after a small number of (expensive) black box function queries.

Figure 4 shows the mean residual in weeks over CPRA for the blood type combination O-AB. The O-AB pair is, in some sense, the easiest pair to match; its donor has the "universal" blood type O, and its patient has no blood type constraints. Indeed, we see that the model estimates the waiting time and quality of this "easy" patient-donor pair quite well. Residuals are small enough that they can be attributed to the stochasticity in the $s = 128$ trials used to test the system.

Figure 5 shows the distribution on the function mapping patient CPRA for the blood type combination AB-O in weeks, the acquisition function (in red) in arbitrary units, and the point at which the acquisition is optimized (the solid red line going down). Figure 6 shows the mean residual in weeks over CPRA for the blood type combination AB-O. We focus on this particular case because the AB-O pair is a complement to the O-AB pair; while the latter is easy to

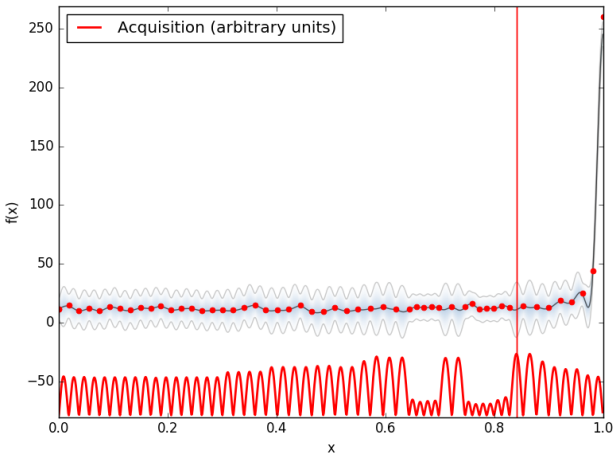

Figure 3: GP for O-type paired donor and AB-type patient (in weeks)

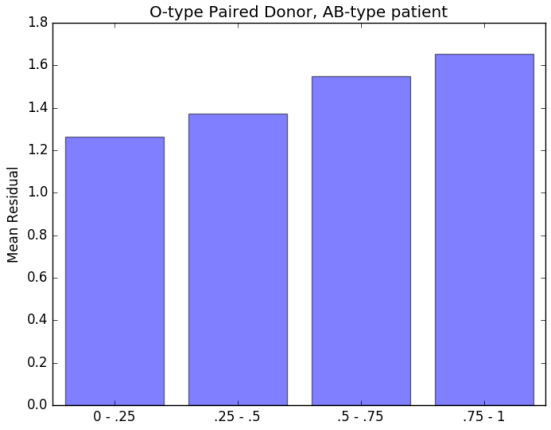

Figure 4: Mean residual in weeks for O-type paired donor and AB-type patient

match, the former has the most constrained donor (type AB donors can only give to type AB patients), and the most constrained patient (type O patients can only receive from type O donors). This increased difficulty in matching led to increased stochasticity in the result, thus giving a higher mean residual.

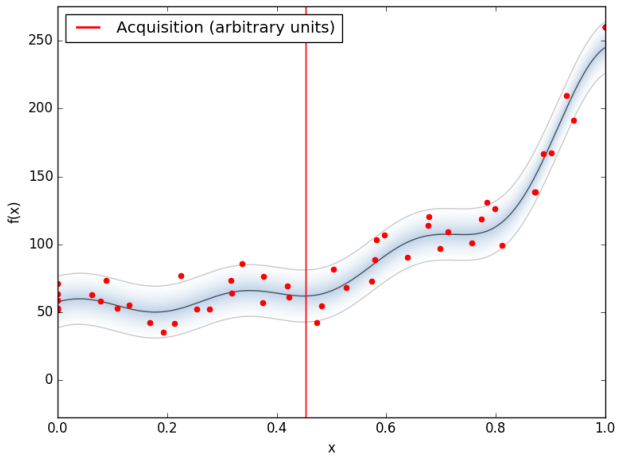

Figure 5: GP for AB-type paired donor and O-type patient (in weeks)

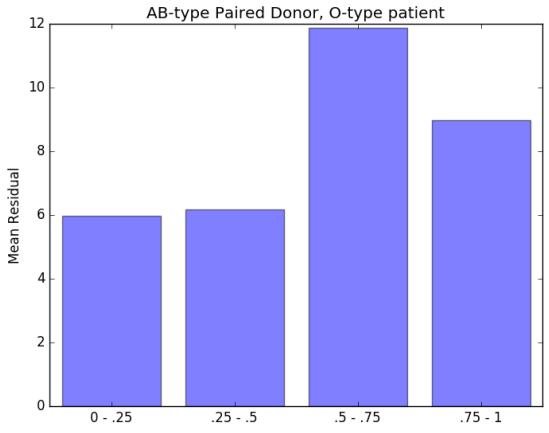

Figure 6: Mean residual in weeks for AB-type paired donor and O-type patient

We performed this experiment for all 16 combinations of patient and donor blood types. Figure 2 gives a high-level quantitative overview of those results; qualitatively, results followed this visualization. In general, higher CPRA leads to greater uncertainty. Similarly, harder to match patients and harder to match donors also lead to greater uncertainty. However, throughout, our method was able to learn a close approximation to the underlying function of interest—even using commodity hardware.

5.1 Discussion

Overall, even with a limited amount of trajectories, the Gaussian Process (GP) provides accurate predictions. As the CPRA increases, the mean residual increases, as the match time output increases in stochasticity with respect to an increase in CPRA. With harder to match blood types (such as the AB-type donor, O-patient donor patient pair), the stochasticity in the result was larger as well, resulting in a higher mean residual. However, as seen in Figure 5, the GP is capable of handling this, by estimating the probability distribution on that value (using a Gaussian prior). Thus, to a certain extent, the GP is capable of handling stochastic outputs.

While this proof of concept demonstrates the promise of this system in a toy environment, before making a policy recommendation or deploying a support tool in practice, we note that:

- the number of trajectories r should be (much) greater, for greatly reduced stochasticity, and thus far smaller mean residuals from the GP to the realistic simulator; and
- the number of features considered should be much higher, and informed by experts in the field.

Yet, given these proof of concept experimental results, we feel confident that—given all F_k—a decision support system can be deployed for use by practitioners, in order to give patients and their willing donors this information on demand.

6 Conclusions & Future Research

This paper presented a principled method to estimate the expected quality of the kidney that a specific patient who enters an exchange will receive, as well as how long it will take to find that match. Knowledge of expected waiting time and organ quality affects medical and insurance decisions. Estimation was performed via a novel Bayesian-optimization-based approach that learns a model of a computationally complex underlying Monte Carlo simulator, which in turn represents a potentially discontinuous function. The method presented generalizes to any additive function of a stochastic (and expensive) simulatable process. With a limited number of expensive simulation trajectories, the model produced reliably accurate results in our proof-of-concept setting, supporting further investigation. With access to fast and accurate sampling, medical professionals could have near-instantaneous access to valuable insight regarding a patient's expected outcome in a kidney exchange system.

The clear future research direction is to determine, via a combination of feature selection methods and expert opinion, the set of features necessary to completely characterize the expected waiting time and kidney quality function our method aims to learn. The model presented, and the proof-of-concept experiments performed, support more intense computational experiments. Similarly, one might use the application of LKDPI presented here to design more socially beneficial mechanisms in the face of strategic agents, perhaps incentivizing agents to perform in a specific way to increase overall social welfare; this area of research, particularly in the context of kidney exchange, is still open (Ashlagi

and Roth 2014; Toulis and Parkes 2015; Hajaj et al. 2015; Blum et al. 2017).

References

Abraham, D.; Blum, A.; and Sandholm, T. 2007. Clearing algorithms for barter exchange markets: Enabling nationwide kidney exchanges. In *Proceedings of the ACM Conference on Electronic Commerce (EC)*, 295–304.

Anderson, R.; Ashlagi, I.; Gamarnik, D.; and Roth, A. E. 2015. Finding long chains in kidney exchange using the traveling salesman problem. *Proc. National Academy of Sciences*.

Andrew, G., and Gao, J. 2007. Scalable training of l_1-regularized log-linear models. In *International Conference on Machine Learning (ICML)*.

Ashlagi, I., and Roth, A. E. 2014. Free riding and participation in large scale, multi-hospital kidney exchange. *Theoretical Economics* 9(3):817–863.

Ashlagi, I.; Gamarnik, D.; Rees, M.; and Roth, A. E. 2017. The need for (long) chains in kidney exchange. Revision requested at Operations Research. Initial version appeared at ACM Conference on Electronic Commerce (EC-12).

Bertsimas, D.; Farias, V. F.; and Trichakis, N. 2013. Fairness, efficiency, and flexibility in organ allocation for kidney transplantation. *Operations Research* 61(1):73–87.

Betancourt, M. 2017. A conceptual introduction to hamiltonian monte carlo.

Biró, P., and Cechlárová, K. 2007. Inapproximability of the kidney exchange problem. *Information Processing Letters* 101(5).

Biró, P.; Manlove, D. F.; and Rizzi, R. 2009. Maximum weight cycle packing in directed graphs, with application to kidney exchange programs. *Discrete Mathematics, Algorithms and Applications* 1(04):499–517.

Blum, A.; Caragiannis, I.; Haghtalab, N.; Procaccia, A. D.; Procaccia, E. B.; and Vaish, R. 2017. Opting into optimal matchings. In *Proceedings of the Symposium on Discrete Algorithms (SODA)*.

Brochu, E.; Cora, V. M.; and De Freitas, N. 2010. A tutorial on bayesian optimization of expensive cost functions, with application to active user modeling and hierarchical reinforcement learning. *arXiv preprint arXiv:1012.2599*.

Dickerson, J. P., and Sandholm, T. 2015. FutureMatch: Combining human value judgments and machine learning to match in dynamic environments. In *AAAI Conference on Artificial Intelligence (AAAI)*, 622–628.

Dickerson, J. P.; Manlove, D.; Plaut, B.; Sandholm, T.; and Trimble, J. 2016. Position-indexed formulations for kidney exchange. In *Proceedings of the ACM Conference on Economics and Computation (EC)*.

Dickerson, J. P.; Procaccia, A. D.; and Sandholm, T. 2013. Failure-aware kidney exchange. In *Proceedings of the ACM Conference on Electronic Commerce (EC)*, 323–340.

Dickerson, J. P.; Procaccia, A. D.; and Sandholm, T. 2014. Price of fairness in kidney exchange. In *International Conference on Autonomous Agents and Multi-Agent Systems (AAMAS)*, 1013–1020.

Ergin, H.; Sönmez, T.; and Ünver, M. U. 2017. Multi-donor organ exchange. Working paper.

Farina, G.; Dickerson, J. P.; and Sandholm, T. 2017. Operation frames and clubs in kidney exchange. In *Proceedings of the International Joint Conference on Artificial Intelligence (IJCAI)*.

Glorie, K. M.; van de Klundert, J. J.; and Wagelmans, A. P. M. 2014. Kidney exchange with long chains: An efficient pricing algorithm for clearing barter exchanges with branch-and-price. *Manufacturing & Service Operations Management (MSOM)* 16(4).

GPyOpt. 2016. GPyOpt: A Bayesian optimization framework in python.

Hajaj, C.; Dickerson, J. P.; Hassidim, A.; Sandholm, T.; and Sarne, D. 2015. Strategy-proof and efficient kidney exchange using a credit mechanism. In *AAAI Conference on Artificial Intelligence (AAAI)*, 921–928.

Jia, Z.; Tang, P.; Wang, R.; and Zhang, H. 2017. Efficient near-optimal algorithms for barter exchange. In *Proceedings of the International Conference on Autonomous Agents and Multiagent Systems (AAMAS)*, 362–370.

Li, J.; Liu, Y.; Huang, L.; and Tang, P. 2014. Egalitarian pairwise kidney exchange: Fast algorithms via linear programming and parametric flow. In *International Conference on Autonomous Agents and Multi-Agent Systems (AAMAS)*, 445–452.

Luo, S.; Tang, P.; Wu, C.; and Zeng, J. 2016. Approximation of barter exchanges with cycle length constraints. *CoRR* abs/1605.08863.

Manlove, D., and O'Malley, G. 2015. Paired and altruistic kidney donation in the UK: Algorithms and experimentation. *ACM Journal of Experimental Algorithmics* 19(1).

Massie, A. B.; Leanza, J.; Fahmy, L.; Chow, E.; Desai, N. M.; Luo, X.; King, E.; Bowring, M.; and Segev, D. 2016. A risk index for living donor kidney transplantation. *American Journal of Transplantation* 16(7):2077–2084.

Mattei, N.; Saffidine, A.; and Walsh, T. 2017. Mechanisms for online organ matching. In *Proceedings of the International Joint Conference on Artificial Intelligence (IJCAI)*.

Montgomery, R.; Gentry, S.; Marks, W. H.; Warren, D. S.; Hiller, J.; Houp, J.; Zachary, A. A.; Melancon, J. K.; Maley, W. R.; Rabb, H.; Simpkins, C.; and Segev, D. L. 2006. Domino paired kidney donation: a strategy to make best use of live non-directed donation. *The Lancet* 368(9533):419–421.

Neuen, B. L.; Taylor, G. E.; Demaio, A. R.; and Perkovic, V. 2013. Global kidney disease. *The Lancet* 382(9900):1243.

Rao, P. S.; Schaubel, D. E.; Guidinger, M. K.; Andreoni, K. A.; Wolfe, R. A.; Merion, R. M.; Port, F. K.; and Sung, R. S. 2009. A comprehensive risk quantification score for deceased donor kidneys: the kidney donor risk index. *Transplantation* 88(2):231–236.

Rees, M.; Kopke, J.; Pelletier, R.; Segev, D.; Rutter, M.; Fabrega, A.; Rogers, J.; Pankewycz, O.; Hiller, J.; Roth, A.; Sandholm, T.; Ünver, U.; and Montgomery, R. 2009. A nonsimultaneous, extended, altruistic-donor chain. *New England Journal of Medicine* 360(11):1096–1101.

Roth, A.; Sönmez, T.; and Ünver, U. 2004. Kidney exchange. *Quarterly Journal of Economics* 119(2):457–488.

Roth, A.; Sönmez, T.; and Ünver, U. 2005a. A kidney exchange clearinghouse in New England. *American Economic Review* 95(2):376–380.

Roth, A.; Sönmez, T.; and Ünver, U. 2005b. Pairwise kidney exchange. *Journal of Economic Theory* 125(2):151–188.

Santos, A. H.; Casey, M. J.; Wen, X.; Zendejas, I.; Rehman, S.; Womer, K. L.; and Andreoni, K. A. 2015. Survival with dialysis versus kidney transplantation in adult hemolytic uremic syndrome patients: A fifteen-year study of the waiting list. *Transplantation* 99(12):2608–2616.

Sönmez, T.; Unver, U.; and Yenmez, M. B. 2017. Incentivized kidney exchange. Tech. report, Boston College Dept. of Economics.

Toulis, P., and Parkes, D. C. 2015. Design and analysis of multi-hospital kidney exchange mechanisms using random graphs. *Games and Economic Behavior* 91(0):360–382.

UNOS. 2015. Revising kidney paired donation pilot program priority points. OPTN/UNOS Public Comment Proposal.